Open Access Research Journal of
Engineering and Technology
Journals home page: https://oarjpublication/journals/oarjet/
ISSN: 2783-0128 (Online)

OARJ OPEN ACCESS RESEARCH JOURNALS

(RESEARCH ARTICLE)

Influence of quartz and marble on the performance of particulate-filled rigid polyurethane foams

Olajesu Favor Olanrewaju [1, 3, *], Isiaka Oluwole Oladele [1, 2], Taiwo Fisayo Omotosho [1], Faruq A. Atilola [1] and Samson Oluwagbenga Adelani [1, 4]

[1] *Department of Metallurgical and Materials Engineering, Federal University of Technology, Akure, PMB 704, Nigeria.*
[2] *Center for Nanomechanics and Tribocorrosion, School of Mining, Metallurgy and Chemical Engineering, University of Johannesburg, Johannesburg 2000, South Africa.*
[3] *Department of Materials Science and Engineering, Iowa State University, Ames, IA, US.*
[4] *Department Materials Science and Engineering, University of Colorado Boulder, 80303, Colorado, USA.*

Open Access Research Journal of Engineering and Technology, 2024, 06(01), 008–025

Publication history: Received on 26 November 2023; revised on 23 January 2024; accepted on 26 January 2024

Article DOI: https://doi.org/10.53022/oarjet.2024.6.1.0011

Abstract

This work was carried out to investigate the roles of quartz and marble on the performance of polyurethane particulate-filled composites. Prior to the mixing, the quartz and marble were pulverized and sieved to obtain an average particle size of less than 90 µm. Polyurethane (PU) was produced from isocyanate and polyol by a two-step method in which marble and quartz particles were incorporated in predetermined proportions. Three different weight ratios were utilized to investigate the physical, chemical, and mechanical behavior of the pristine rigid polyurethane foam (RPUF) and the marble and quartz-filled RPUF using analytical equipment such as FTIR, XRF, and SEM. The mechanical properties were performed according to the ASTM standards, where the compressive and flexural strengths were investigated using the universal testing machine. Overall, the RPUF shows the hydroxyl bands, while the principal elements of fillers are Calcium and Silicon. It was discovered from the results that adding these fillers improved the mechanical properties of the filled samples, where the compressive strength was enhanced.

Keywords: Polyurethane; Foam; Quartz; Marble; Composites

1. Introduction

Polyurethane (PU) originated from the synthesis of Wurtz in 1849, after which Otto Bayer's group discovered PU in 1937, which they named 'Das DI-Isocganat-Poluadditions verfahren. PUs are produced by combining isocyanate groups with hydroxyl groups of polyols. Initially, PU's were thought worthless, but are now a key component of many everyday life products and one of the most utilized polymer classes. In 2018, PU ranked sixth among the polymer classes in production, with about 25 million metric tons of production recorded in 2019 and a global estimated consumption of 79 billion USD in the year 2021 [1]–[3]. However, the market values of PUs are always fluctuating because the main constituent for producing PU (polyols and poly-isocyanate) depends on global petroleum prices [4]. Since the initial production of PU, it has gained substantial prominence in engineering due to excellent moldability [5].

Also, the simple production route of a reaction between diisocyanate (diphenyl isocyanate) and polyester diol (ethoxylated cycloalkyl amine /polyol) made PU the choice polymer for applications such as architecture, aerospace, automobiles, thermal insulation, PU-based foams, adhesives, wastewater treatment, military, space, and the biomedical field [6], [7]. Consequently, as the global population grows, there are increased consumption levels and waste production [8]. The most consumed PU class are PU foams (PUF), and the high levels of consumption birth the need for improved sustainability, excellent thermal insulation, enhanced durability, and economical attractiveness [9]. These

* Corresponding author: Olajesu Favor Olanrewaju

Copyright © 2024 Author(s) retain the copyright of this article. This article is published under the terms of the Creative Commons Attribution Liscense 4.0.

improvements are achieved by altering the composition-microstructure-property relationship, mostly achieved in PU by various additives.

The concentration and finetuning action of several additives in the reaction between polyols, isocyanates, and blowing agents dictate the final properties of PU [10]. The additives include catalysts, surfactants, and flame retardants [11]. The additives used in producing PU include catalysts, blowing agents, and crosslinkers. The addition of a catalyst accelerates the reaction under low-temperature conditions, blowing agents and surfactants aid the production and control of PU foam cell structure, while cross-linkers (chain extenders) improve the mechanical properties such as tensile strength and hardness by structural modification of the RPUF. Other additives that can influence the properties of RPUF are plasticizers that reduce the hardness of the material, fillers that improve stiffness and tensile strength, and flame retardants that reduce the susceptibility of RPUF to burning or catching fire [5], [12]–[15].

In the biomedical field, PU is versatile for producing medical devices with excellent mechanical properties and hemocompatibility [16]. Other properties of PU include excellent toughness and abrasion resistance, making it applicable in producing solid tire wheels, body panels, and bumper components in the automobile industry [17]. PU-based products such as PU foams, elastomers, adhesives, PU labs, molded foams, carpet backing, and coating are utilized for their thermal resistivity, good mechanical properties in compression, acoustic, and chemical properties [18], [19]. One of the most widely utilized PU-based products is PU foam, renowned for lightweight applications and contributing to about 70% of global PU consumption; the remaining 30% are elastomers, adhesives, and other PUs [11]. PU foams are subdivided into flexible (60%) and rigid (40%) categories with ever-growing, well-established production technologies [20]. The rigid PU foam (RPUF) has an effective temperature range of (−235 °C to 150 °C) with good strength, especially for cryogenic and space applications. The thermal conductivity of RPUF is (k = 0.02 W/m·K under ambient temperature conditions), which is relatively low but has a high strength-to-density ratio (8–9 kPa/kg/m^3) [21].

RPUF can cover intricate shapes as a coating material by using the spray method, but the adhesion is dependent on the chemical structure of the polymer matrix and is expected to be rigid at ambient temperature conditions but flexible at cryogenic conditions. This makes RPUF one of the excellent thermal insulation materials available [22], [23]. Also, in the cosmetic industry, RPUF pumices are considered a good substitute for natural pumices because of their considerable size, shape, and color control during production. Additionally, RPUF pumices are fungi-resistant, bacterial-resistant, and non-toxic for human skin [24]. Although RPUF possesses excellent properties, it is not without flaws, which include dimensional instability, low mechanical properties, high thermal conductivity undesirable in cryogenic conditions [25], [26], and significant plastic deformation in certain temperature-influenced conditions [27]. Hence, researchers have proven that adding filler materials in RPUF can substantially improve certain properties in the RPUF. The properties altered by adding filler materials include thermal, water uptake and retention, dimensional stability, fire resistance, and photodegradation [28].

Alterations in the RPUF morphology, such as increased anisotropy, cause the reported property improvement. Significant improvement in mechanical properties because of glass fiber additions for automotive industry applications was reported by Cziolonka et al. [28] and Barczewski et al. [29]. Natural fibers are termed suitable reinforcing materials because of their accessibility, cost-effectiveness, lightweightness, and biodegradability. At times, natural fibers are degraded by the high manufacturing temperatures of polymers, resulting in defects in the RPUF structure. Silva et al. [30] confirmed that cellulose filler for RPUF decreased cell size and thermal conductivity, caused no significant improvement in thermo-oxidative stability and mechanical properties, and caused fungi growth. Also, natural fibers can be hydrophilic, forming agglomerates of undesirable distribution within the matrix of the RPUF [25], making researchers investigate other reinforcing materials for RPUF. Yu et al. [31] reported improved tensile, compressive, and mechanical properties from fiber reinforcements. The improvement in the mechanical properties results from the capacity of fibers to infiltrate voids.

The report from Oh et al. [32] shows that replacing fibers with Kevlar pulps improves the mechanical properties significantly, and the optimal properties are obtained when the cell volume distribution is the lowest. Increasing the quantity of Kevlar pulp above the threshold value leads to no significant improvement besides being an intercellular filler and increasing insulation. Similarly, Omotoyinbo et al. [33] showed that adding dolomite and kaolin altered the absorption peaks and improved the hardness, flexural, and compressive strength of RPUF. Felspar addition to RPUF was also found to alter the absorption peaks with improved microstructure and hydrophobicity but negatively affected the rheological properties and the sulfonic acid groups [34].

Researchers have used different techniques to quantify the mechanical properties of RPUF. The properties such as hardness, compressive, tensile, and flexural strength measure a material's resistance to localized/surface plastic deformation/indentation [35], [36]. The simplest technique for a hardness test measurement uses an indenter to make plastically deforming indents on the sample surface [37]. The RPUF samples can be tested using a micro-hardness intender according to the ASTM D2240-00 standard [33], [38]. Other mechanical properties such as tensile, compressive, flexural, and impact strength can be carried out on a universal testing machine and impact testing machine [33]. Currently, researchers are working on improving the properties of PU foams to match the rising demands of the populace by engineering the properties of PU foams. Also, researchers are seeking alternatives for creating transformation routes to improve the potential of natural minerals to improve the properties of PU foams. A profound effort has been made toward manufacturing PU-based composites with improved properties and functional applications [39]. Combining PU foams with other materials can improve its use in applications such as wound dressing, tissue engineering, drug delivery, biosensing, and automobile applications [40].

The effect of quartz (SiO_2) and marble ($CaCO_3$) on RPUF has been researched by several researchers [41]–[43]. However, none of this prior research quantified the rheological effect of adding quartz and marble to RPUF. Also, prior research only considered synthetic SiO_2 and $CaCO_3$, not the naturally sourced mineral form. There is an increasing need for sustainability, which requires using natural filler materials as substitutes for synthetic fillers in PU foam production, hence creating environmentally friendly and less costly production routes. Therefore, this research investigates the production, characterization, and examination of PU foams reinforced with natural filler (quartz and marble) and highlights their physical impact on the rheological properties of RPUF. X-ray Fluorescence (XRF) spectroscopy confirmed the elemental composition of the quartz and marble. Fourier Transform Infrared was used to confirm the urethane linkages, while scanning electron microscopy (SEM) was used to examine the morphological alterations in the samples. In addition, the mechanical impact of quartz and marble fillers was confirmed using compressive and flexural strength tests.

2. Material and methods

In this research, three separate closed-cell PU foams were produced from the mixture of polyol and isocyanate for the experimental analysis: the pure PU foam, the marble ($CaCO_3$) particles reinforced PU foam, and the quartz (SiO_2) particles reinforced PU foam. Three weight fractions (3, 5, and 7 wt.%) of the quartz and the marble were used to fully articulate the particles' influence on PU foams. The utilization of three samples offers valuable statistical information on estimating the changes in the mechanical properties of the PU foams. This provides material property distribution for statistical analysis, as seen in previous studies [44]. The curing and reactivity of PU are caused by isocyanate, while polyols cause flexible long segments.

2.1. Preparation of RPUF composites

The isocyanate and polyols were purchased from a Chemical and Allied Company in Lagos State, Nigeria. Naturally sourced marble and quartz were washed, dried, crushed, and pulverized using a centrifugal ball mill and then sieved with a mesh of 90 μm, and the marble and quartz undersize were used. A control sample of RPUF was made, which contains 0 % of the filler particles. Three samples with proportions 3, 5, and 7 wt% of the marble fillers were made to test the effect of the marble filler on PU foam. This step was also repeated for the quartz-filled samples. The RPUFs were prepared by mechanically stirring the isocyanate, polyol, and filler particles mixed in a two-step process. The first step is adding varying amounts (0 wt.%, 3 wt.%, 5 wt.%, and 7 wt.%) of marble and quartz particles to 60g of isocyanate and stirring to evenly disperse the particles in the mixture. The second step is adding 60g of polyols to the mixture for direct reaction and stirring for about 10 seconds, after which the mixture was poured into an open mold. The mixing ratio of 1:1 was maintained for the isocyanate and polyols.

The time-dependent rheological properties were measured as the reaction proceeded using a stopwatch. The two-step process is done according to the works of Zieleniewska et al. [24], Omotoyinbo et al. [33], and Omotoyinbo et al.[34], and Nunes de Oliveira Júnior et al. [45]. An open mold with dimensions 81 mm × 100 mm × 130 mm was used for this research. After the resin had cured with sufficient rigidity, the foam was de-molded and allowed to cure completely for 24 hours. A specimen size of 3.0×10^3 mm was cut out of each sample for experimental analysis.

2.2. Measurement and Characterization

The rheological properties (cream, gel, rise, and tack-free time) of the RPUF were recorded with a digital stopwatch. An SEM (JEOL JSM-760 0F) was used in the morphological characterization of the RPUF composite. For SEM analysis, the samples were made electrically conductive by gold sputter-coating and imaged with an accelerating voltage of 15kV. The infrared band shift of the RPUF samples was evaluated using the Infrared spectrometer Varian 660 MidIR Dual

MCT/DTGS Bundle with ATR. Before the FTIR experiments, the samples were desiccated for 24 hours with potassium (KBr) slices. Afterward, the RPUF scans were made using the spectrophotometric analyzer to confirm the functional chemical groups present in the samples. The volume, density, and weight changes were observed for 30 minutes. Equation (1) was used in calculating the density.

$$Density = \frac{mass}{volume} \text{.....(1)}$$

The water absorption experiment was conducted on all the samples by soaking the samples in water for 24 hours under room temperature (300 K) conditions. After 24 hours, the samples were taken out and wiped clean of any water remnant, and the weights were instantaneously measured using a digital scale. Similar experiments were repeated for 48 hours and 72 hours by instantaneously returning the samples to the immersion medium. The initial weights (w_i) and final weights (w_f) after each period of all the samples were measured and recorded. The % moisture content was calculated using equation (2).

$$\%\ moisture\ content = \frac{w_f - w_i}{w_i} \times 100\% \text{.....(2)}$$

The X-ray fluorescence (XRF) analysis of the samples was performed on the filled RPUF to determine the elemental composition using the Energy Dispersive Spectrometer (EDX3600B). The chemical composition of the filled RPUF was determined by using 0.5 g of each RPUF sample, pressed using lithium tetraborate (flux) to produce an evenly dispersed solution. Then, the atoms in the samples are excited by X-ray beams on the sample, causing the electrons to jump into a higher orbital level for identification.

2.3. Mechanical Properties

The mechanical properties of the pristine RPUF and filled RPUF were estimated using compression and flexural test analysis. The compressive strength was investigated using two test specimens each for the pristine analysis and two test specimens for each of the weight percentages for the RPUF-filled samples. For the compression samples, cubic dimensions of length 3 cm were made, and the compression test analysis was done using a universal testing machine (3369 INSTRON) working simultaneously with blue-hill software according to the ASTM 1621 standard [33], [46]. The software generated the maximum compressive stress and strain values, the fracture stress and strain values, and the compressive yield stress values for the three samples. The flexural strength was evaluated to test the sample's resistance to bending/deflection or the stress at which the material fails under bending stresses [47], [48]. The flexural stress analysis was also performed using the universal testing machine (3369 INSTRON) according to ASTM D790-03 standard [33], [49]. The flexural strength was investigated using three test specimens each for the pristine sample and each composition of the filler materials. The flexural test samples are of cuboid geometry and dimensions 15 × 5 × 0.5 cm using a three-point bend test at a 5 mm/min strain rate.

3. Results and discussion

3.1. Estimation of the rheological properties

Cream time is the bench time between mixing the components of the RPUF and when the mixture turns creamy or when there is an observable homogeneous creamy/milky texture in the polymeric mixture. The gel time is defined as the interval that allows the RPUF to turn into a gel, resulting from the cross-linking reactions of the mixture. The gel time is also the period of bubble formation accompanied by a rising foamy reaction, after which a pasty substance is formed from the homogeneous state when the gel state is achieved. The gel time can notably affect the rise time because, for evenly dispersed filler particles in the RPUF, the gel time increases considerably as the particles create nucleation sites for bubble formation and reduced cell size. The rise time comes immediately after the gel time, which is accompanied by an expansion of the mixture resulting from the continuous stirring for producing RPUF. The presence of filler particles in the RPUF alters the almost instantaneous rise time. The time taken for the full rise of RPUF is directly proportional to the curing time. The importance of the rise time is that it indicates the end of the RPUF formation process [50]. Also, the rise time directly influences the tack-free time, which is the time taken between the end of the rise time and the RPUF becoming completely non-sticky and completely cured. The cream, gel, and rise time are usually within seconds, measured using a stopwatch. The cream, gel, rise, and tack-free time for the RPUF are shown in Figure 1.

Overall, the cream time was found to increase upon the addition of marble and quartz particles. This is attributed to the delay caused by the presence of particles in the structural formation of PU. The resultant effect of the increased cream time is the increased time for curing in the RPUF-filled samples. This implies that the smaller the number of particles,

the higher the contact between the fillers and the isocyanate, resulting in lower cream, gel, rise, and tack-free time for the RPUF. Increasing the weight percentage increases the chance of the particles encountering each other, therefore decreasing the RPUF contact with the filler particles, thereby increasing the cream time and reducing the reaction temperature [28]. In RPUF filled with marble, the cream, gel, rise, and tack-free time increased from 3 wt.% to 5 wt.% particles before a drop at 7 wt.%. For the quartz-filled RPUF, the cream, gel, and rise time was highest at 7 wt.%, while the tack-free time was highest at 3 wt.%. The results show that the increased time depends on the physical and chemical properties and the weight percentage of constituents (filler particles) of the reaction mixture. The cream, gel, rise, and tack-free time for marble particles is higher than that of quartz particles, even for the same quantity of filler particles.

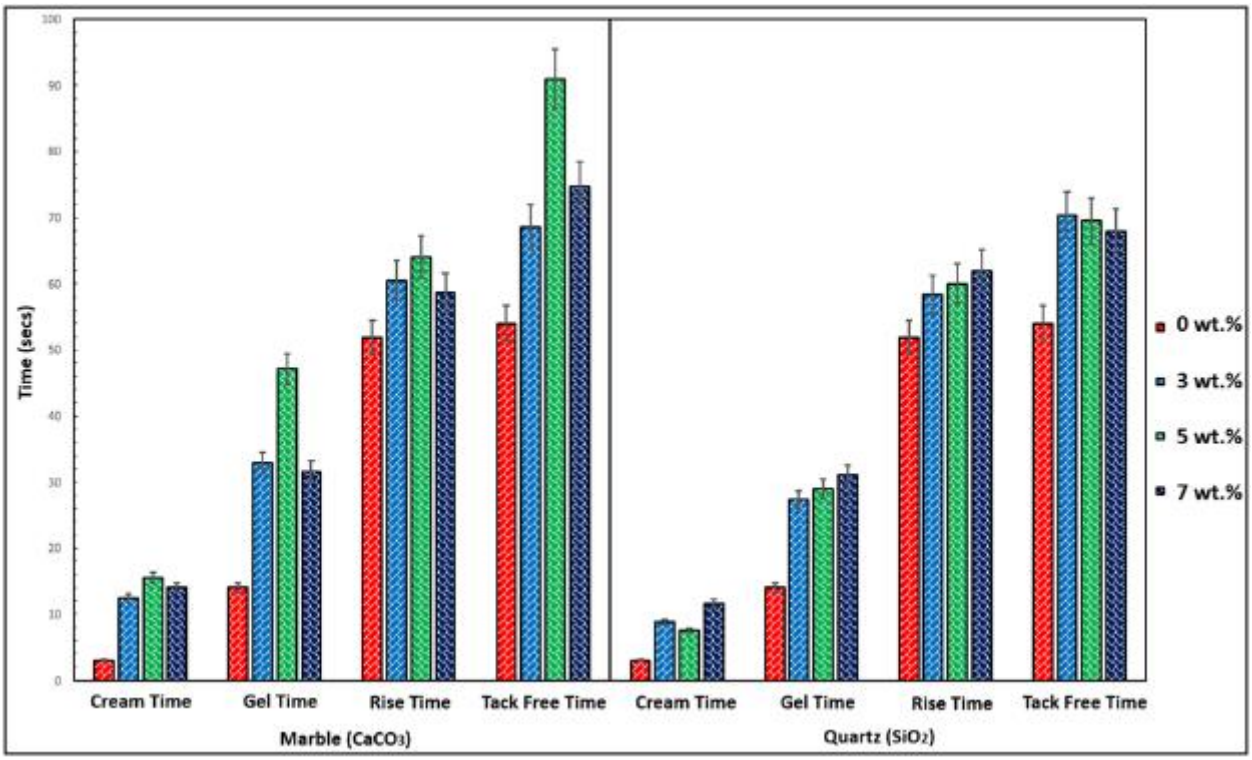

Figure 1 The cream, gel, rise, and tack-free time for RPUF composite

3.2. Fourier Transform Infrared (FTIR) Analysis

The FTIR analysis was performed on the pure RPUF and RPUF filled with marble and quartz particles to assess the chemical bonding of the PU. The absorbed wavelength in the FTIR spectrum indicates the presence of the chemical bonds present in the sample. The pristine RPUF spectrum is shown in Table 1 and Figure 2. Likewise, the FTIR spectra of the marble-filled RPUF and quartz-filled RPUF are shown in Tables 2 and 3 and Figures 3 and 4, respectively. According to the work of Oliviero et al. [51], the absence of a 2230 cm^{-1} band in the spectrum shows the complete consumption of the isocyanate groups, signifying that the reaction in the pristine RPUF, marble-filled RPUF, and the quartz-filled RPUF is complete. Also, there is a vibrational range between 1600 - 1720 cm^{-1} band, representing the characterization peaks of PU foams.

The pristine RPUF shows O-H stretching and stretching vibration peaks at 2910 cm^{-1} and 3098 cm^{-1}, respectively. C-H stretching vibration of the polyol is evident at the peak of 2834 cm^{-1} band, C=N stretching, S-H stretching, CH_2 asymmetric variation, S=O asymmetric stretching, C-O-C asymmetric stretching, O-S-O stretching, and C-Cl stretching vibration are represented at peaks of 1942 cm^{-1}, 1710 cm^{-1}, 1608 cm^{-1}, 1398 cm^{-1}, 1099 cm^{-1}, 1050 cm^{-1}, and 528 cm^{-1}, respectively. The -CH bending vibrations are also notable at the 926 cm^{-1} band peak. Similarly, the O-H stretching bond is present in the marble-filled RPUF at the 3100 cm^{-1} band peak. Other peak bands are at 3099 cm^{-1}, 3050 cm^{-1}, 1999 cm^{-1}, 1231 cm^{-1}, 800 cm^{-1}, and 618 cm^{-1}, representing the N-H stretching, -C=C-stretching, C=N stretching, C-N-C stretching vibration, Si-O stretching vibration, and Si-O-Si bending vibration respectively. For the quartz-filled RPUF, the O-H stretching peaks are at 2481 cm^{-1}, while other important peaks such as C-H stretching, C-N-C stretching vibration, C-O-C asymmetric stretching, O=C=O Stretching, C=O stretching, C=C aromatic stretching, C-Cl stretching vibration, are at 2313 cm^{-1}, 1215 cm^{-1}, 962 cm^{-1}, 920 cm^{-1}, 861 cm^{-1}, and 620 cm^{-1} band peaks, respectively.

According to Bandekar and Kilma [52], the expected Infrared peaks of RPUF are carbonyl H-bonds, ether H-bonds, and urethane alkoxyl groups. The notable O-H bonds in the examined RPUF and the composites belong to the carboxyl group. Many factors can cause the shifting of C-O-C asymmetric stretching bands, including alterations in the C-O bonds, H-bond formation between the NH groups, and urethane alkoxy oxygen. The H-bonding of urethane C-O-C groups with the NH group can cause increased shifts. It is also possible that C-O-C asymmetric stretching regions with lower wave numbers are products of the carbonyl oxygen displacement by the alkoxy oxygen in the NH group. The absorbance of the pristine RPUF for the O-H stretching vibration is higher than the marble-filled and quartz-filled. This implies that the specific frequencies related to the atom-to-atom vibrational bond energies in RPUF were altered by adding marble and quartz-filler particles, thereby altering the characteristic fingerprint spectrum. This means that the marble and quartz fillers bonded with the structure of RFUP, implying that the adhesive force between the fillers and the matrix is strong. The absorbance shows that the concentration of the RFUP has reduced and has been replaced by the filler particles of marble and quartz.

In the work of Trovati et al. [7], the excess O-H trifunctional hydroxyl molecules with one free group decrease the cross-linking degrees. Excess O-H bonds are considered unfavorable for the formation of RPUF because the polymer structure of RPUF does not have variable degrees of branching compared to the flexible counterpart. It is noticed that silica bands in the filled RPUF are from the chemical constituents of the filler particles of marble and quartz, responsible for sulphonic group degradation.

Table 1 FTIR spectrum values for pristine RPUF

Run	Peak (cm^{-1})	Transmittance (%)	Absorbance	Assignment
1	3098.22	61.35	0.2122	O-H Stretching vibration
2	3095.11	48.20	0.3170	-C=C- stretching
3	3043.40	28.94	0.5385	H-NH stretching
4	2910.25	16.47	0.7833	O-H stretching
5	2834.02	48.11	0.3178	C-H stretching vibration of polyol
6	1942.61	85.73	0.0669	C=N stretching
7	1710.26	81.35	0.0896	S-H stretching
8	1608.71	52.41	0.2800	CH2 asymmetric variation
9	1498.37	20.03	0.6983	deformation CH2 + C=C of the aromatic ring
10	1450.11	20.71	0.6838	C-H bending of unsaturated methylene groups.
11	1398.47	73.95	0.1311	S=O asymmetric Stretching
12	1099.20	73.04	0.1364	C-O-C asymmetric stretching
13	1050.22	64.39	0.1912	O-S-O stretching
14	926.34	72.16	0.1417	-CH bending vibration to substitute in alkenes ad aromatics
15	771.42	28.74	0.5415	-CH2 bending
16	708.15	4.10	0.3872	C=C aromatic stretching
17	528.73	60.41	0.2188	C-Cl stretching vibration

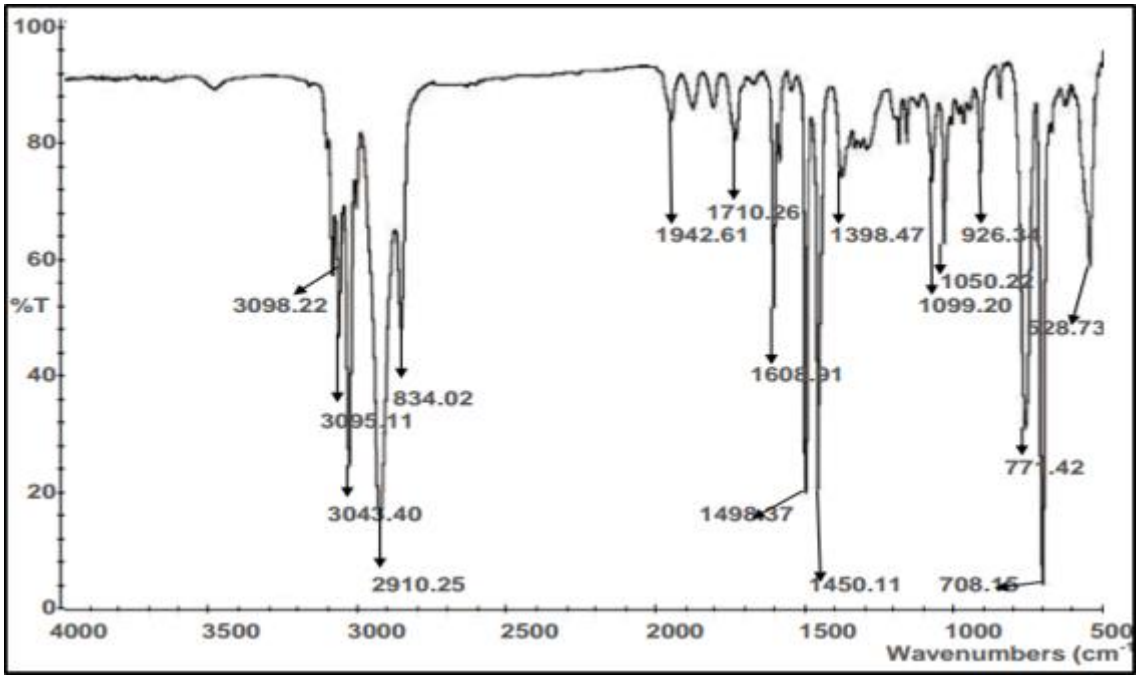

Figure 2 Infrared Spectra of the pristine RPUF

Table 2 FTIR spectrum values for marble-filled polyurethane foam

Run	Peak (cm^{-1})	Transmittance (%)	Absorbance	Assignment
1	3100.96	72.54	0.1394	O-H Stretching
2	3099.25	72.77	0.1381	N-H Stretching
3	3050.08	72.83	0.1377	-C=C- stretching
4	2963.28	12.02	0.9201	symmetric stretching- the vibration of the aliphatic –CH2 group
5	2899.39	36.51	0.4376	C-H stretching of – CH2
6	1999.74	80.26	0.0955	C=N stretching
7	1792.81	40.15	0.3963	-C-O stretching
8	1690.77	44.56	0.3511	H-O-H bending vibrations of adsorbed water molecules.
9	1593.14	36.39	0.4390	O=C=O stretching
10	1500.26	28.21	0.5496	CH2 symmetric stretching
11	1448.86	44.37	0.3529	C-H bending of unsaturated methylene groups.
12	1390.72	46.18	0.3355	deformation CH2 + C=C of the aromatic ring
13	1231.64	52.81	0.2773	C-N-C stretching vibration
14	1100.00	56.80	0.2457	O-H deformation and Si-O-Si modes.
15	820.53	52.64	0.2787	C-O-C symmetric stretching
16	800.02	4.57	1.3401	Si-O stretching vibration
17	618.22	68.24	0.1660	Si-O-Si bending vibration

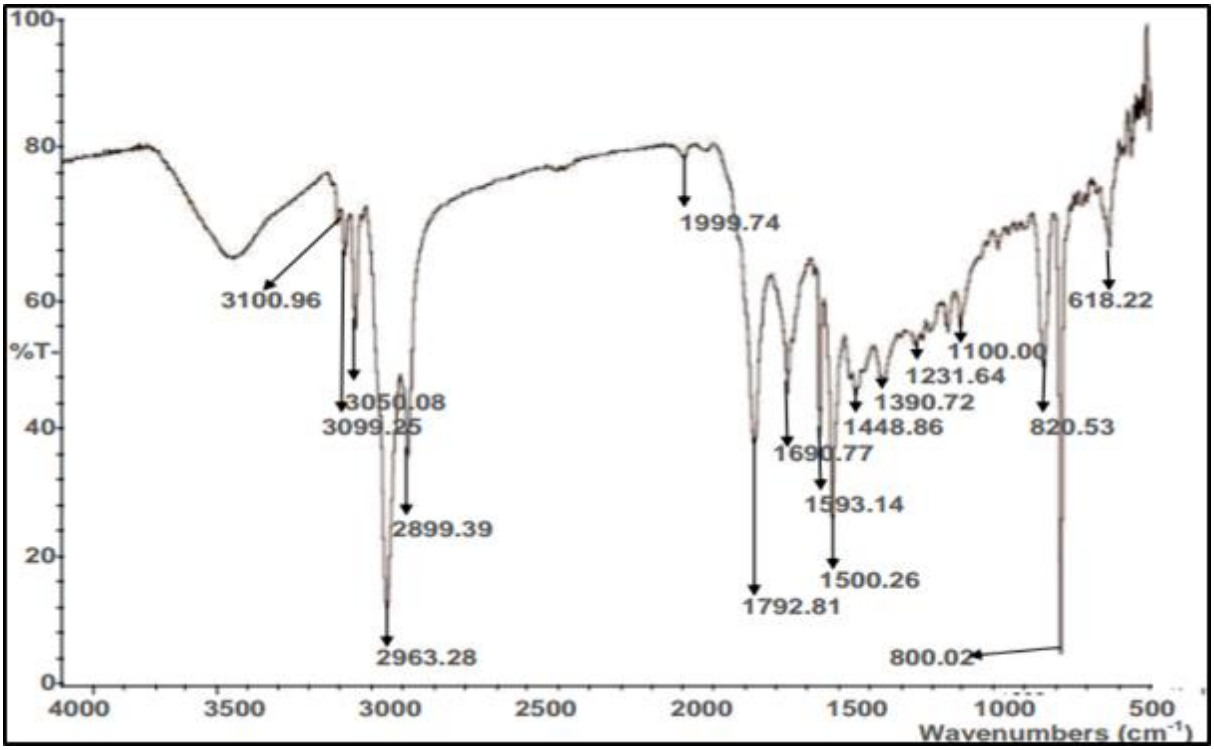

Figure 3 Infrared Spectra of the marble-filled RPUF

Table 3 FTIR spectrum values for quartz-filled RPUF

Run	Peak (cm^{-1})	Transmittance (%)	Absorbance	Assignment
1	2481.31	85.72	0.0669	O-H Stretching vibration
2	2383.72	24.50	0.6108	C-H, N-H Stretching
3	2313.55	98.41	0.3558	C-H stretching
4	1708.32	16.20	0.0070	-C-O stretching
5	1215.41	64.98	0.7905	C-N-C stretching vibration
6	962.21	75.90	0.1906	C-O-C asymmetric stretching
7	920.26	75.90	0.1198	O=C=O Stretching
8	861.23	61.31	0.2125	C=O stretching
9	848.91	35.02	0.4557	C=N stretching
10	800.30	56.23	0.2500	C-O-C symmetric stretching
11	736.21	85.14	0.0699	C=C aromatic stretching
12	682.31	52.58	0.2792	The heteroatom vibration frequency of sulfur and nitrogen
13	620.03	83.49	0.0784	C-Cl stretching vibration

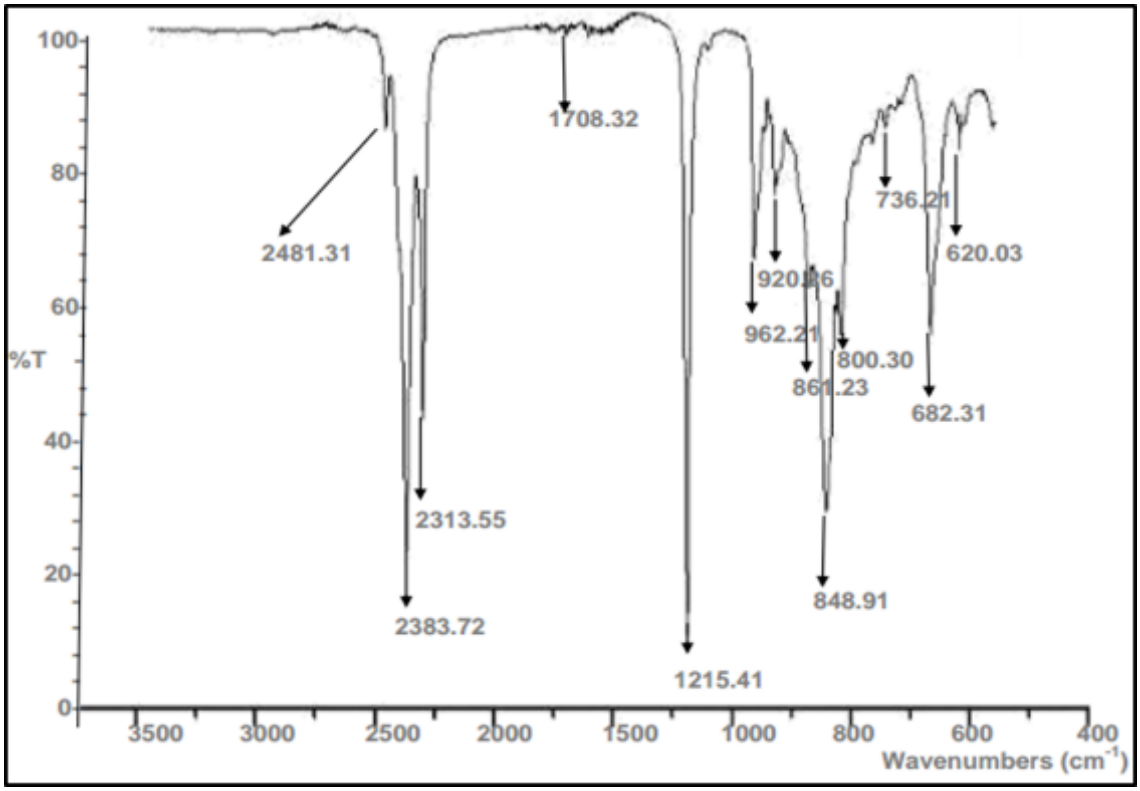

Figure 4 Infrared Spectra of the quartz-filled RPUF

3.3. The XRF Analysis

Figures 5 and 6 show the XRF analysis for the marble and quartz filler, respectively. The XRF gives the quantitative composition of the elements present in both fillers. In the marble filler, the principal elements are Ca and Si, while in quartz, the principal elements are Si, as shown in Tables 4 and 5. The principal elemental compositional values obtained for both filler materials match prior research [53]–[57]. These results show that quartz and marble contain other important elements that enhance the mechanical strength of the RPUF foams.

Table 4 XRF results for marble filler

Element	Intensity	Content
Mg	0.0000	0.0000
Al	0.0103	2.7625
Si	0.1403	15.1012
P	0.0055	0.2609
S	0.0117	0.9189
K	0.0778	6.3357
Ca	0.0399	28.6230
Ti	0.0011	0.0214
V	0.0002	0.0097
Cr	0.0001	0.0000
Mn	0.0006	0.0398
Co	0.0019	0.0653
Fe	0.0536	5.1745

Ni	0.0007	0.0382
Cu	0.0016	0.0348
Zn	0.0025	0.0849
As	0.0008	0.0000
Pb	0.0005	0.0171
W	0.0002	0.0359
Au	0.0000	0.0000
Ag	0.0000	0.0000
Nb	0.0018	0.0165
Mo	0.0043	0.1653
Cd	0.0000	0.0000
Sn	0.0067	1.2478
Sb	0.0086	1.0788

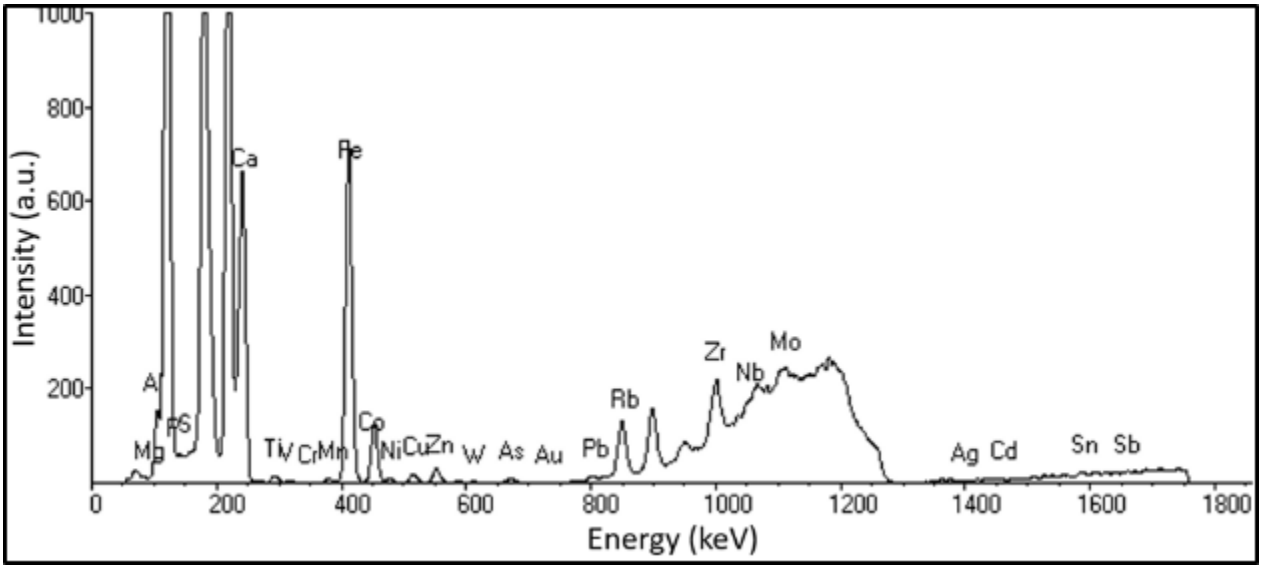

Figure 5 The XRF peaks for marble fillers

Table 5 XRF results for quartz-filler

Element	**Intensity**	**Content**
Mg	0.0000	0.0000
Al	0.0152	3.8339
Si	0.5803	75.6552
P	0.0048	0.2271
S	0.0047	0.3212
K	0.0041	0.3265

Ca	0.0038	0.0509
Ti	0.0000	0.0000
V	0.0001	0.0040
Cr	0.0000	0.0000
Mn	0.0004	0.0247
Co	0.0000	0.0000
Fe	0.0042	0.4764
Ni	0.0008	0.0452
Cu	0.0015	0.0325
Zn	0.0022	0.0738
As	0.0008	0.0000
Pb	0.0007	0.0261
W	0.0001	0.0000
Au	0.0001	0.0541
Ag	0.0000	0.0000
Nb	0.0000	0.0000
Mo	0.0020	0.2349
Cd	0.0000	0.0000
Sn	0.0049	0.9155
Sb	0.0069	0.8584

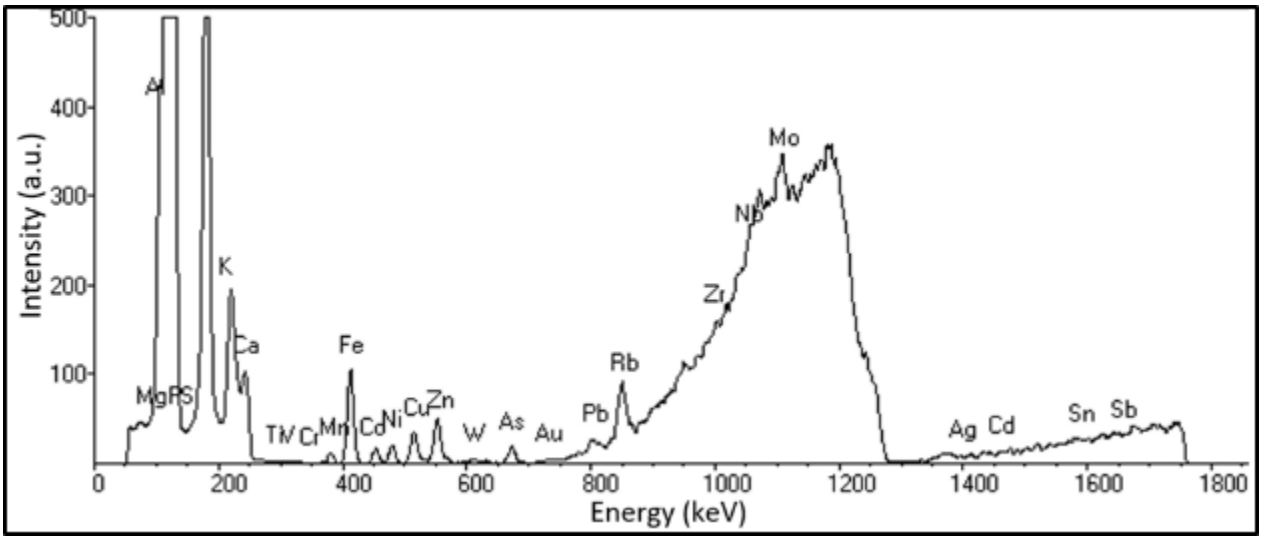

Figure 6 The XRF peaks for the quartz filler

3.4. RPUF Morphology

The morphology of the pristine RPUF and filled RPUF was imaged using SEM. The images showed that the pristine RPUF has thin, irregular pattern walls with an average size of about 200 µm. There are observable broken walls in the unfilled RPUF (Figure 7a). The addition of marble-filler particles shows thick walls with more irregularly broken walls (Figure 7b), while the quartz particle almost fills the voids present in the structure of RPUF (Figure 7c). The result implies that

filler materials can completely alter the morphological properties of RPUF. While small amounts of filler materials can improve mechanical properties, high concentrations can lead to cell rupture. Choosing the right binding agent and the filler quantity is important, as it controls cell growth uniformity of nucleated cells [51]. Note the presence of filler materials also reduces the roughness and porosity of RPUF and improves the adhesion between the fillers and the matrix [33], [34].

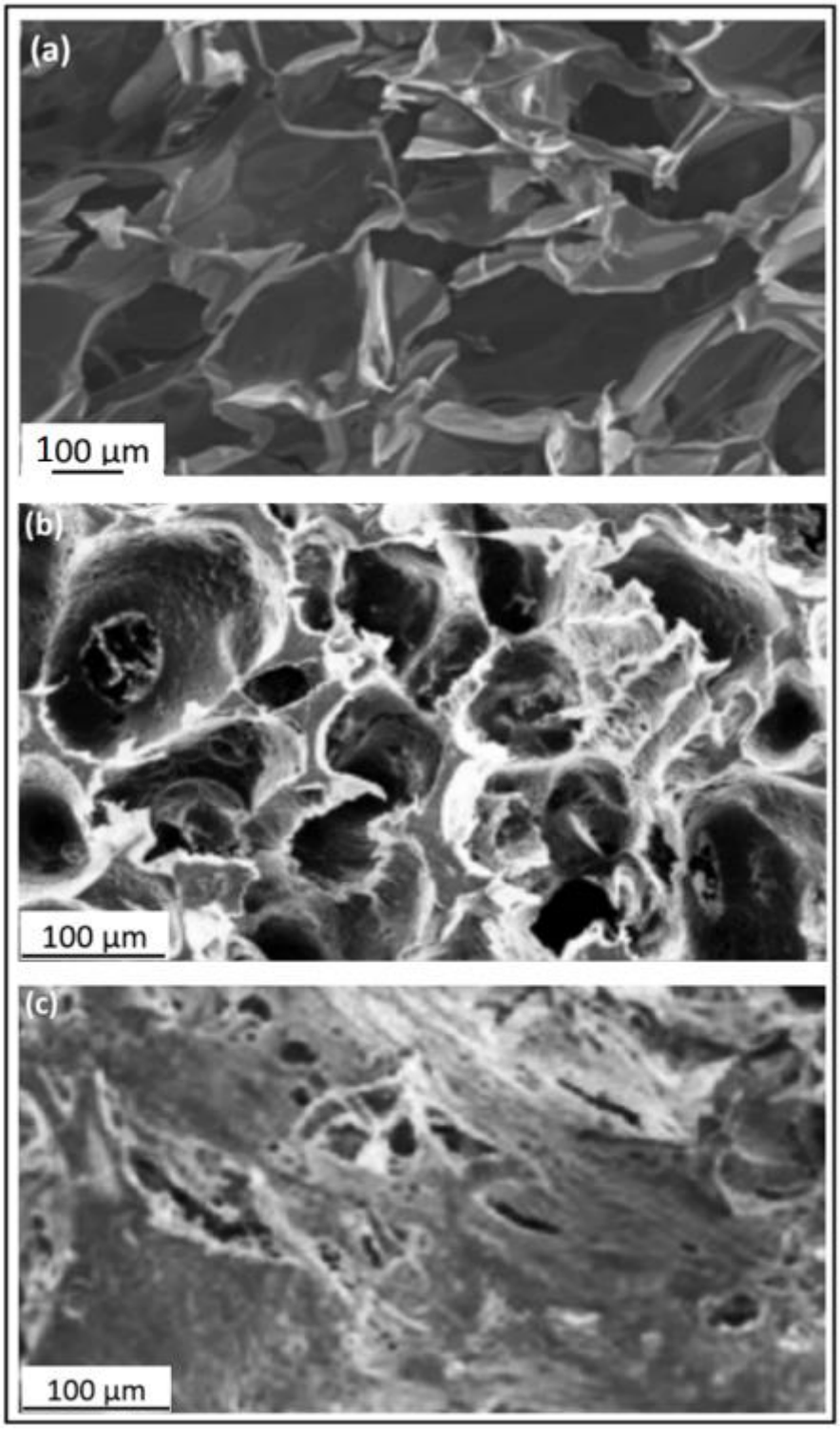

Figure 7 The SEM images of RPUF (a) pristine, (b) marble-filled, and (c) quartz-filled (SEM Images taken at different magnifications to reveal cell structures)

3.5. Water Absorptivity

The water absorptivity results in Figure 8 show that adding filler materials increases the water absorptivity. Overall, quartz-filled RPUF shows more absorptivity compared to the marble-filled RPUF. The samples soaked for 72 hours had the highest absorptivity for the control samples, gradually increasing as the immersion time increased. For the immersion time of 24 hours (M_1), the 3 wt.% of the marble-filled RPUF had the highest absorptivity value, while the 7 wt.% of the quartz-filled RPUF had the highest absorptivity value. For the immersion time of 48 hours (M_2), the 5 wt.% of the marble-filled RPUF had the highest absorptivity value, while the 3 wt.% of the quartz-filled RPUF had the highest absorptivity value. Finally, for the immersion time of 72 hours (M_3), the 7 wt.% of the marble-filled RPUF had the highest absorptivity value, while the 5 wt.% of the quartz-filled RPUF had the highest absorptivity value. The 3 wt.% and 5 wt.% marble-filled RPUF has lower absorptivity at 72 hours than the pristine RPUF, showing the capacity for applicability in hydrophobic applications.

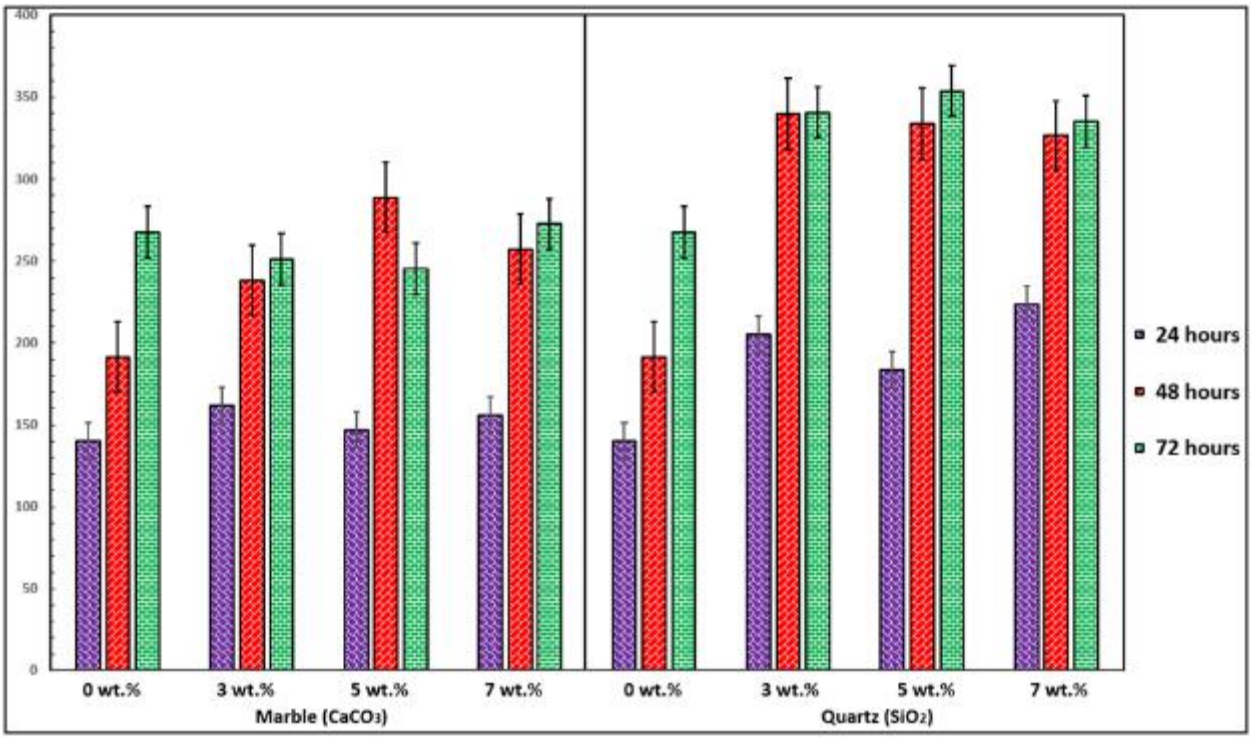

Figure 8 The water absorptivity of RPUF

3.6. Density of RPUF

The density of the filled RPUF increased in a non-consistent manner. In the marble-filled RPUF, the mass increased from 0 wt. % to 3 wt.%, but reduced from 3 wt. % to 5 wt.%, before another noticeable increase at 7 wt.%. This irregular pattern continued in the density. The quartz-filled sample showed a consistently decreasing value as the weight percentage of the filler increased and still maintained an irregular pattern in the other samples. The quantitative values of the density of the pristine and filled RPUF samples are shown in Figure 9. This inconsistent difference in density was also noticed by Ramamoorthy et al. [58]. In this research, it is believed that the inconsistencies in the density are caused by uneven particle distribution and clustering of the filler materials in the RPUF. Also, it is important to note that this can also be caused by air entrapment and porosities within the RPUF-filled samples. There are other potential causes for the inconsistencies in the density but which are highly unlikely for this study; this includes variations in particle size and shape, incompatibility between the RPUF phase and filler materials, the difference in the processing parameters, and agglomeration of filler materials.

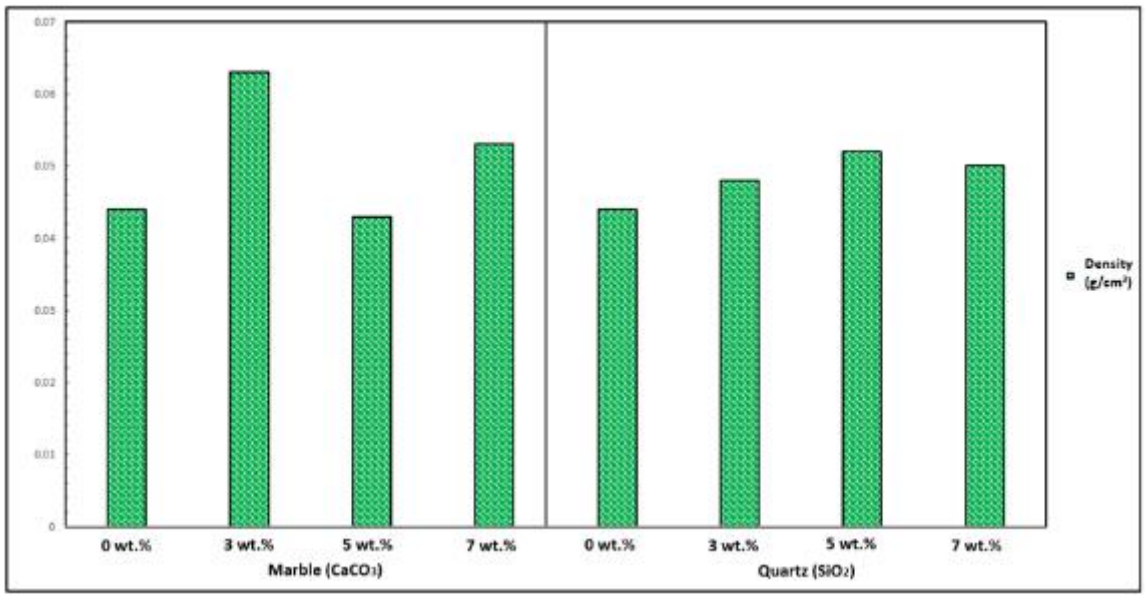

Figure 9 The density of pristine and filled RPUF samples

3.7. Mechanical Behavior of RPUF

The compressive analysis of the filled and the pristine RPUF samples is shown in Figure 10. The table shows the Maximum Compressive Stress (M.C.S), Maximum Compressive Strain (M.C.St), Compressive Stress at Break/Fracture (C.S.B), Compressive Strain at Break/Fracture (C.St.B), and Compressive Yield Stress (C.Y.S). Overall, the filler materials enhanced the compressive strength of the RPUF and increased the compressive strain to fracture as well. The quartz-filled RPUF shows more compressive strain to failure compared to the marble-filled RPUF. The flexural analysis shown in Figure 11 shows that the flexural strength of the unfilled RPUF was observed to be greater than both filled RPUF samples. This implies that an increase in the filler materials leads to a corresponding decrease in the ductility of the samples but increased compressive strength. This result is similar to that obtained by Omotoyinbo et al. [33], Zhao et al. [59], and Jia et al. [60].

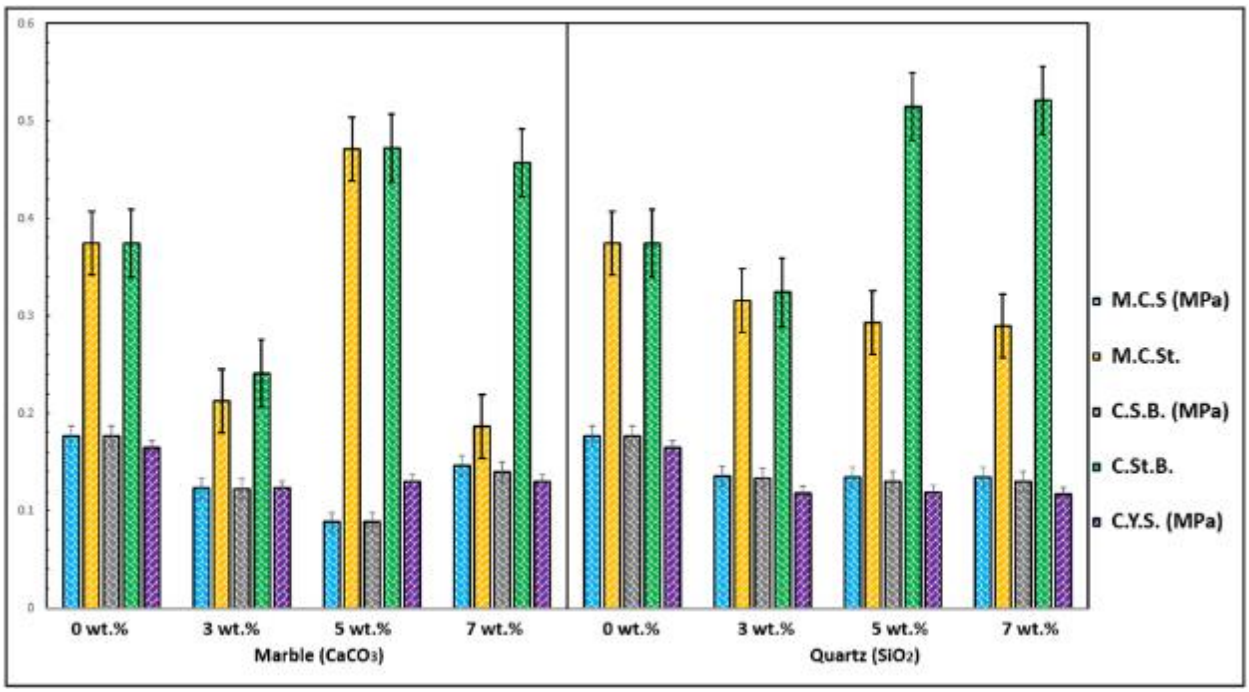

Figure 10 The compressive analysis of the pristine and filled RPUF samples

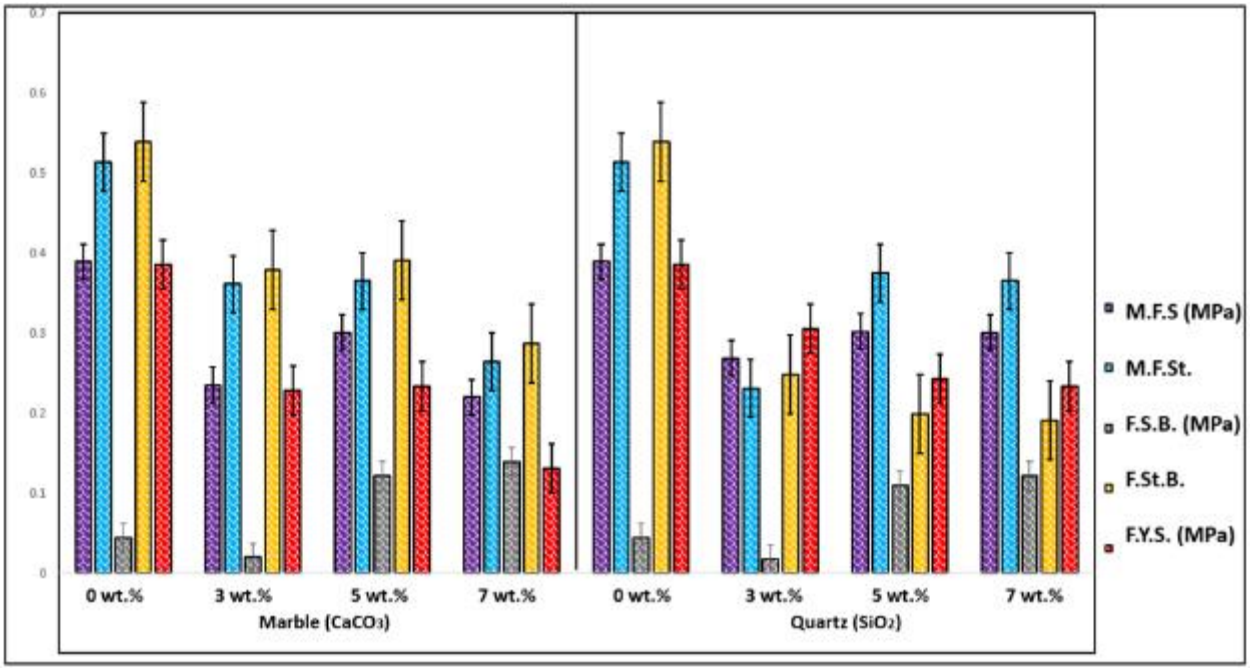

Figure 11 The flexural analysis of the pristine and filled RPUF samples

4. Conclusion

In this research, several RPUF foams were made using isocyanate and polyol, which were reinforced with marble and quartz-fille particles. After this, the physical, chemical, and mechanical properties of the filled RPUF were investigated. The results of FTIR analysis showed the expected presence of the O-H bands in all the RPUF samples, and the filler materials altered the absorbance of the sample, meaning the filler materials were properly bonded to the RPUF. The principal elements in the marble fillers are Calcium and Silicon, and the quartz -fillers is Silicon, as shown by the XRF analysis. The increase in cream, gel, rise, and, subsequently, tack-free time was because of the reaction occurring within the matrix is partly because the filler particles are encountering each other instead of directly with the molecules of isocyanate. The SEM analysis also showed that the filler particles are embedded in the gaps between the foam structure, thereby improving the strength of the RPUF composite. The overall mechanical strength of the RPUF samples was improved by adding filler materials, making marble and quartz good reinforcing materials for industrial applications.

In conclusion, the results of this study show that quartz and marble-filled RPUF show potential for futuristic applications in replacing synthetic alternatives as filler materials. These substitutive capabilities contribute to the global mission of sustainability by making lightweight vehicles that increase fuel efficiency. Further studies can be conducted to investigate the thermal conductivity of the quartz-filled and marble-filled RPUF.

Compliance with ethical standards

Disclosure of conflict of interest

No conflict of interest to be disclosed.

References

[1] O. Bayer, Das Di-Isocyanat-Polyadditionsverfahren (Polyurethane),*Angewandte Chemie*, vol. 59, no. 9, pp. 257–272, Sep. 1947, doi: 10.1002/ange.19470590901.

[2] N. Gama, A. Ferreira, and A. Barros-Timmons, Polyurethane Foams: Past, Present, and Future, *Materials*, vol. 11, no. 10, p. 1841, Sep. 2018, doi: 10.3390/ma11101841.

[3] C. Liang *et al.*, "Material Flows of Polyurethane in the United States," *Environ Sci Technol*, vol. 55, no. 20, pp. 14215–14224, Oct. 2021, doi: 10.1021/acs.est.1c03654.

[4] H. T. T. Tran, A. D. K. Deshan, W. Doherty, D. Rackemann, and L. Moghaddam, "Production of rigid bio-based polyurethane foams from sugarcane bagasse, *Ind Crops Prod*, vol. 188, p. 115578, Nov. 2022, doi: 10.1016/j.indcrop.2022.115578.

[5] A. Das and P. Mahanwar, A brief discussion on advances in polyurethane applications, *Advanced Industrial and Engineering Polymer Research*, vol. 3, no. 3, pp. 93–101, Jul. 2020, doi: 10.1016/j.aiepr.2020.07.002.

[6] C. Li *et al.*, "Fabrication and properties of antimicrobial flexible nanocomposite polyurethane foams with in situ generated copper nanoparticles," *Journal of Materials Research and Technology*, vol. 19, pp. 3603–3615, Jul. 2022, doi: 10.1016/j.jmrt.2022.06.115.

[7] G. Trovati, E. A. Sanches, S. C. Neto, Y. P. Mascarenhas, and G. O. Chierice, "Characterization of polyurethane resins by FTIR, TGA, and XRD," *J Appl Polym Sci*, vol. 115, no. 1, pp. 263–268, Jan. 2010, doi: 10.1002/app.31096.

[8] D. Głowacz-Czerwonka, P. Zakrzewska, M. Oleksy, K. Pielichowska, M. Kuźnia, and T. Telejko, "The influence of biowaste-based fillers on the mechanical and fire properties of rigid polyurethane foams," *Sustainable Materials and Technologies*, vol. 36, p. e00610, Jul. 2023, doi: 10.1016/j.susmat.2023.e00610.

[9] G. Avar, U. Meier-Westhues, H. Casselmann, and D. Achten, "Polyurethanes," in *Polymer Science: A Comprehensive Reference*, Elsevier, 2012, pp. 411–441. doi: 10.1016/B978-0-444-53349-4.00275-2.

[10] D. S. Kaikade and A. S. Sabnis, "Polyurethane foams from vegetable oil-based polyols: a review," *Polymer Bulletin*, vol. 80, no. 3, pp. 2239–2261, Mar. 2023, doi: 10.1007/s00289-022-04155-9.

[11] F. Recupido *et al.*, "Rigid composite bio-based polyurethane foams: From synthesis to LCA analysis," *Polymer (Guildf)*, vol. 267, p. 125674, Feb. 2023, doi: 10.1016/j.polymer.2023.125674.

[12] H. Sheikhy, M. Shahidzadeh, B. Ramezanzadeh, and F. Noroozi, "Studying the effects of chain extenders chemical structures on the adhesion and mechanical properties of a polyurethane adhesive," *Journal of Industrial and Engineering Chemistry*, vol. 19, no. 6, pp. 1949–1955, Nov. 2013, doi: 10.1016/j.jiec.2013.03.008.

[13] N. Taheri and S. Sayyahi, "Effect of clay loading on the structural and mechanical properties of organoclay/HDI-based thermoplastic polyurethane nanocomposites," *e-Polymers*, vol. 16, no. 1, pp. 65–73, Jan. 2016, doi: 10.1515/epoly-2015-0130.

[14] Y. Savelyev *et al.*, "Preparation and characterization of new biologically active polyurethane foams," *Materials Science and Engineering: C*, vol. 45, pp. 127–135, Dec. 2014, doi: 10.1016/j.msec.2014.08.068.

[15] H. Sheikhy, M. Shahidzadeh, B. Ramezanzadeh, and F. Noroozi, "Studying the effects of chain extenders chemical structures on the adhesion and mechanical properties of a polyurethane adhesive," *Journal of Industrial and Engineering Chemistry*, vol. 19, no. 6, pp. 1949–1955, Nov. 2013, doi: 10.1016/j.jiec.2013.03.008.

[16] L.-C. Xu and C. A. Siedlecki, Antibacterial polyurethanes, in *Advances in Polyurethane Biomaterials*, Elsevier, 2016, pp. 247–284. doi: 10.1016/B978-0-08-100614-6.00009-3.

[17] S.-J. Park and M.-K. Seo, Element and Processing, 2011, pp. 431–499. doi: 10.1016/B978-0-12-375049-5.00006-2.

[18] X. Qian, Q. Liu, L. Zhang, H. Li, J. Liu, and S. Yan, Synthesis of reactive DOPO-based flame retardant and its application in rigid polyisocyanurate-polyurethane foam, *Polym Degrad Stab*, vol. 197, p. 109852, Mar. 2022, doi: 10.1016/j.polymdegradstab.2022.109852.

[19] C. H. Zhang, Z. Hu, G. Gao, S. Zhao, and Y. D. Huang, Damping behavior and acoustic performance of polyurethane/lead zirconate titanate ceramic composites," *Materials & Design (1980-2015)*, vol. 46, pp. 503–510, Apr. 2013, doi: 10.1016/j.matdes.2012.10.015.

[20] N. Gama, A. Ferreira, and A. Barros-Timmons, "Polyurethane Foams: Past, Present, and Future," *Materials*, vol. 11, no. 10, p. 1841, Sep. 2018, doi: 10.3390/ma11101841.

[21] K. Uram, A. Prociak, L. Vevere, R. Pomilovskis, U. Cabulis, and M. Kirpluks, Natural Oil-Based Rigid Polyurethane Foam Thermal Insulation Applicable at Cryogenic Temperatures, *Polymers (Basel)*, vol. 13, no. 24, p. 4276, Dec. 2021, doi: 10.3390/polym13244276.

[22] Y. Jiang, H. Yang, X. Lin, S. Xiang, X. Feng, and C. Wan, "Surface Flame-Retardant Systems of Rigid Polyurethane Foams: An Overview," *Materials*, vol. 16, no. 7, p. 2728, Mar. 2023, doi: 10.3390/ma16072728.

[23] Y. Hu, Z. Zhou, S. Li, D. Yang, S. Zhang, and Y. Hou, Flame Retarded Rigid Polyurethane Foams Composites Modified by Aluminum Diethylphosphinate and Expanded Graphite, *Front Mater*, vol. 7, Feb. 2021, doi: 10.3389/fmats.2020.629284.

[24] M. Zieleniewska *et al.*, Development and applicational evaluation of the rigid polyurethane foam composites with egg shell waste," *Polym Degrad Stab*, vol. 132, pp. 78–86, Oct. 2016, doi: 10.1016/j.polymdegradstab.2016.02.030.

[25] B. Sture, L. Vevere, M. Kirpluks, D. Godina, A. Fridrihsone, and U. Cabulis, Polyurethane Foam Composites Reinforced with Renewable Fillers for Cryogenic Insulation, *Polymers (Basel)*, vol. 13, no. 23, p. 4089, Nov. 2021, doi: 10.3390/polym13234089.

[26] W. Zhou, C. Bo, P. Jia, Y. Zhou, and M. Zhang, Effects of Tung Oil-Based Polyols on the Thermal Stability, Flame Retardancy, and Mechanical Properties of Rigid Polyurethane Foam," *Polymers (Basel)*, vol. 11, no. 1, p. 45, Dec. 2018, doi: 10.3390/polym11010045.

[27] J. Wang, C. Zhang, Y. Deng, and P. Zhang, A Review of Research on the Effect of Temperature on the Properties of Polyurethane Foams, *Polymers (Basel)*, vol. 14, no. 21, p. 4586, Oct. 2022, doi: 10.3390/polym14214586.

[28] S. Członka, E. Fischer Kerche, R. Motta Neves, A. Strąkowska, and K. Strzelec, "Bio-Based Rigid Polyurethane Foam Composites Reinforced with Bleached Curauá Fiber," *Int J Mol Sci*, vol. 22, no. 20, p. 11203, Oct. 2021, doi: 10.3390/ijms222011203.

[29] M. Barczewski *et al.*, Rigid polyurethane foams modified with thermoset polyester-glass fiber composite waste, *Polym Test*, vol. 81, p. 106190, Jan. 2020, doi: 10.1016/j.polymertesting.2019.106190.

[30] M. C. Silva, J. A. Takahashi, D. Chaussy, M. N. Belgacem, and G. G. Silva, "Composites of rigid polyurethane foam and cellulose fiber residue, *J Appl Polym Sci*, p. n/a-n/a, 2010, doi: 10.1002/app.32281.

[31] Y. H. Yu, I. Choi, S. Nam, and D. G. Lee, "Cryogenic characteristics of chopped glass fiber reinforced polyurethane foam, *Compos Struct*, vol. 107, pp. 476–481, Jan. 2014, doi: 10.1016/j.compstruct.2013.08.017.

[32] J.-H. Oh, J.-H. Bae, J.-H. Kim, C.-S. Lee, and J.-M. Lee, Effects of Kevlar pulp on the enhancement of cryogenic mechanical properties of polyurethane foam, *Polym Test*, vol. 80, p. 106093, Dec. 2019, doi: 10.1016/j.polymertesting.2019.106093.

[33] J. A. Omotoyinbo *et al.*, Comparative investigation of the influence of kaolin and dolomite on the properties of polyurethane foam, *Manuf Rev (Les Ulis)*, vol. 8, p. 27, Nov. 2021, doi: 10.1051/mfreview/2021025.

[34] J. A. Omotoyinbo *et al.*, MICROSTRUCTURAL CHARACTERISATION, RHEOLOGICAL AND WATER ABSORPTION PROPERTIES OF FILLED POLYURETHANE FOAM, *FUTA JOURNAL OF ENGINEERING AND ENGINEERING TECHNOLOGY*, vol. 16, no. 1, pp. 33–43, May 2022, doi: 10.51459/futajeet.2022.16.1.359.

[35] E. G. Mota and K. Subramani, Nanotechnology in operative dentistry, in *Emerging Nanotechnologies in Dentistry*, Elsevier, 2018, pp. 59–82. doi: 10.1016/B978-0-12-812291-4.00004-2.

[36] A. A. WHITE and S. M. BEST, Properties and characterisation of bone repair materials, in *Bone Repair Biomaterials*, Elsevier, 2009, pp. 121–153. doi: 10.1533/9781845696610.2.121.

[37] R. C. Bradt, Ceramic Crystals and Polycrystals, Hardness of, in *Encyclopedia of Materials: Science and Technology*, Elsevier, 2001, pp. 1045–1051. doi: 10.1016/B0-08-043152-6/00193-5.

[38] L. P. Djukic, D. C. Rodgers, and M. T. Herath, 3.16 Design, Certification and Field Use of Lightweight Highly Chemically Resistant Bulk Liquid Transport Tanks, in *Comprehensive Composite Materials II*, Elsevier, 2018, pp. 439–459. doi: 10.1016/B978-0-12-803581-8.10345-5.

[39] N. B. Shelke, R. K. Nagarale, and S. G. Kumbar, Polyurethanes, in *Natural and Synthetic Biomedical Polymers*, Elsevier, 2014, pp. 123–144. doi: 10.1016/B978-0-12-396983-5.00007-7.

[40] J. Hu and L. Tan, Polyurethane Composites and Nanocomposites for Biomedical Applications," in *Polyurethane Polymers*, Elsevier, 2017, pp. 477–498. doi: 10.1016/B978-0-12-804065-2.00016-4.

[41] M. Thirumal, D. Khastgir, N. K. Singha, B. S. Manjunath, and Y. P. Naik, Mechanical, Morphological and Thermal Properties of Rigid Polyurethane Foam: Effect of the Fillers, *Cellular Polymers*, vol. 26, no. 4, pp. 245–259, Jul. 2007, doi: 10.1177/026248930702600402.

[42] H. Choe, J. H. Lee, and J. H. Kim, Polyurethane composite foams including CaCO3 fillers for enhanced sound absorption and compression properties," *Compos Sci Technol*, vol. 194, p. 108153, Jul. 2020, doi: 10.1016/j.compscitech.2020.108153.

[43] M. H. Moghim, M. Keshavarz, and S. M. Zebarjad, Effect of SiO2 nanoparticles on compression behavior of flexible polyurethane foam, *Polymer Bulletin*, vol. 76, no. 1, pp. 227–239, Jan. 2019, doi: 10.1007/s00289-018-2384-0.

[44] L. B. Bezek, C. A. Chatham, D. A. Dillard, and C. B. Williams, Mechanical properties of tissue-mimicking composites formed by material jetting additive manufacturing, *J Mech Behav Biomed Mater*, vol. 125, p. 104938, Jan. 2022, doi: 10.1016/j.jmbbm.2021.104938.

[45] J. Nunes de Oliveira Júnior, F. Perissé Duarte Lopes, N. Tonini Simonassi, D. Souza, S. Neves Monteiro, and C. M. Fontes Vieira, "Evaluation of the physical properties of composite panels with eucalyptus sawdust waste and castor oil-based polyurethane, *Journal of Materials Research and Technology*, vol. 23, pp. 1084–1093, Mar. 2023, doi: 10.1016/j.jmrt.2023.01.067.

[46] N. Elbers, C. K. Ranaweera, M. Ionescu, X. Wan, P. K. Kahol, and R. K. Gupta, Synthesis of Novel Biobased Polyol via Thiol-Ene Chemistry for Rigid Polyurethane Foams," *J Renew Mater*, vol. 5, no. 1, pp. 74–83, Jan. 2017, doi: 10.7569/JRM.2017.634137.

[47] P. Noorunnisa Khanam, M. A. Al-Maadeed, and P. Naseema Khanam, "Silk as a reinforcement in polymer matrix composites, in *Advances in Silk Science and Technology*, Elsevier, 2015, pp. 143–170. doi: 10.1016/B978-1-78242-311-9.00008-2.

[48] A. M. N. Azammi *et al.*, Characterization studies of biopolymeric matrix and cellulose fibres based composites related to functionalized fibre-matrix interface," in *Interfaces in Particle and Fibre Reinforced Composites*, Elsevier, 2020, pp. 29–93. doi: 10.1016/B978-0-08-102665-6.00003-0.

[49] A. International and files indexed by mero, Standard Test Methods for Flexural Properties of Unreinforced and Reinforced Plastics and Electrical Insulating Materials 1, 2019. [Online]. Available: https://www.researchgate.net/publication/330713407

[50] M. S. Suleman *et al.*, Synthesis and Characterization of Flexible and Rigid Polyurethane Foam, 2014. [Online]. Available: https://www.researchgate.net/publication/287980438

[51] M. Oliviero, M. Stanzione, M. D'Auria, L. Sorrentino, S. Iannace, and L. Verdolotti, Vegetable Tannin as a Sustainable UV Stabilizer for Polyurethane Foams, *Polymers (Basel)*, vol. 11, no. 3, p. 480, Mar. 2019, doi: 10.3390/polym11030480.

[52] J. Bandekar and S. Klima, FT-IR spectroscopic studies of polyurethanes Part I. Bonding between urethane C-O-C groups and the NH Groups, 1991.

[53] K. Diouri, A. Chaqroune, A. Kherbeche, J. Bentama, and A. Lahrichi, "Kinetics of yellow dye adsorption onto marble powder sorbents, *Journal of Materials and Environmental Science*, vol. 6, pp. 79–92, Jan. 2015.

[54] M. Zumrawi and E. Abdalla, *stabilization of expansive soil using marble waste powder* . 2018.

[55] H. Ahmed, *Characteristics of Micro & Nano Composite from Marble& Granite Wastes*. 2017.

[56] G. M. A. Wahab, M. Gouda, and G. Ibrahim, "Study of physical and mechanical properties for some of Eastern Desert dimension marble and granite utilized in building decoration, *Ain Shams Engineering Journal*, vol. 10, no. 4, pp. 907–915, Dec. 2019, doi: 10.1016/j.asej.2019.07.003.

[57] S. Fares, A. Yassene, A. Ashour, M. Abu-Assy, M. Abd, and E. Rahman, Natural radioactivity and the resulting radiation doses in some kinds of commercially marble collected from different quarries and factories in Egypt," *Nat Sci (Irvine)*, vol. 03, Jan. 2011, doi: 10.4236/ns.2011.310115.

[58] S. K. Ramamoorthy, F. Bakare, R. Herrmann, and M. Skrifvars, Performance of biocomposites from surface modified regenerated cellulose fibers and lactic acid thermoset bioresin," *Cellulose*, vol. 22, no. 4, pp. 2507–2528, Aug. 2015, doi: 10.1007/s10570-015-0643-x.

[59] H. Zhao, W. She, D. Shi, W. Wu, Q. Zhang, and R. K. Y. Li, Polyurethane/POSS nanocomposites for superior hydrophobicity and high ductility, *Compos B Eng*, vol. 177, p. 107441, Nov. 2019, doi: 10.1016/j.compositesb.2019.107441.

[60] Z. Jia, G. Yuan, X. Feng, Y. Zou, and J. Yu, Shear properties of polyurethane ductile adhesive at low temperatures under high strain rate conditions, *Compos B Eng*, vol. 156, pp. 292–302, Jan. 2019, doi: 10.1016/j.compositesb.2018.08.060.